CHAPTER II

LITERATURE REVIEW

2.1 Overview

Geophysical exploration methods have been applied in engineering, geological, and environmental fields for particular purposes. The recent research on the in-situ seismic testing is focused on the surface wave method. A fundamental framework of surface wave has been initiated from the application of ultrasonic testing method for concrete characterization (Viktorov, 1967). Then, the idea has been extended to the earth structure investigation by seismologists (Ewing et al., 1957; Dorman et al., 1960; Dorman and Ewing, 1962; Bullen, 1963; Knopoff, 1972; Kovach, 1978; Keilis-Borok et al., 1989; Mokhart et al., 1988; Al-Eqabi and Herrmann, 1993; Herrman and Al-Eqabi, 1991).

A robust modification has been introduced to civil engineering application by Jones (1958, 1962) and Ballard (1964). It was know as Steady State Rayleigh Method (SSRM), which uses a mechanical vibrator to generate the Rayleigh or Love waves and a single receiver to detect the signal. Subsequently, the success of this work led to the extension of another approach (Spectral Analysis of Surface Waves Method, SASWM) by using a couple of receivers instead of a single one (Nazarian and Stokoe 1984, 1986; Stokoe and Nazarian, 1985; Stokoe et al, 1988, 1994). This method is based on the principle of SSRM; however, the field measurement is somehow easier. Nevertheless, some drawbacks were recognized from the previous method. It remains a time consuming task in data acquisition and is easily disturbed by noise generated from traffic, construction site, factor, etc. A better way to get rid of those weaknesses is to employ a number of receivers to capture the arrival of waves generated from the impact sources. It is nominated as Multichannel Analysis of Surface Wave Method MASWM (Park et al., 1999; Xia et al., 1999; Foti, 2000). The coherency of the incident waves travelling from trace-to-trace allows us to distinguish it from the ambient noise. In the next section, a brief review of useful methods is presented. In this chapter, the two fundamental methods, i.e., SSRM and SASWM, are demonstrated including the field setup and data processing part.

2.2 Steady State Rayleigh Method (SSRM)

The basic concept of this technique is to search for the wavelengths corresponding to the different input frequencies from the source. It enables us to compute the phase velocity of Rayleigh or Love waves that can be used to construct the dispersion curve. From the field measurement, the vibrator is placed vertically perpendicular to the free surface so that the majority of energy transmitted from the source is Rayleigh wave. Love waves can be obtained by setting the vibrator in the position that ready to produce the signal in horizontal direction and the receiver is directed to detect it. The common signal used in the experiment is Rayleigh waves. The procedure of SSRM is illustrated in figure 2.1.

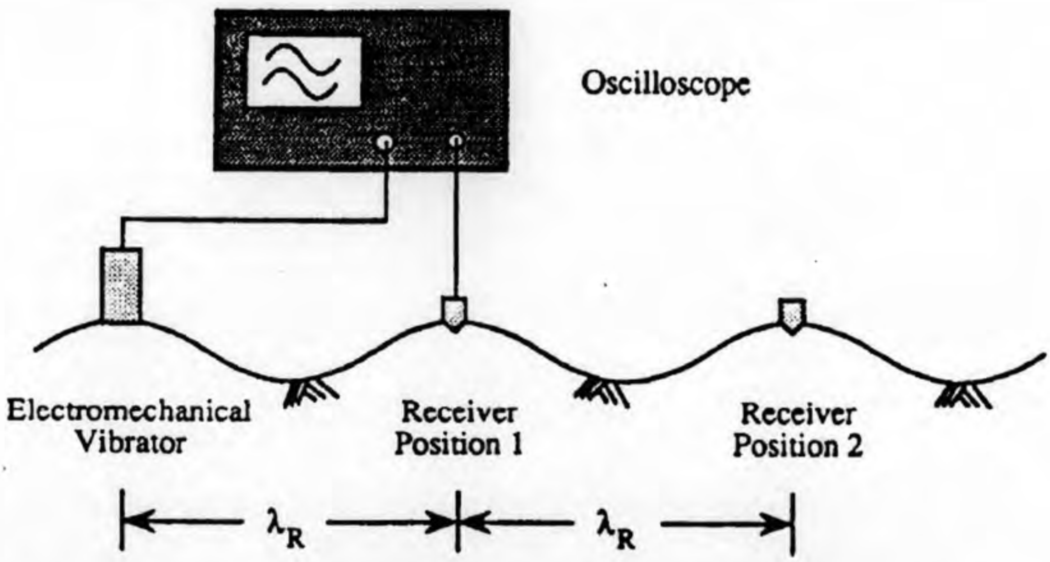

Figure 2-1 Field Procedure for Steady State Rayleigh Method (After Rix 1988)

The input signals with frequencies (f) from the vertical sinusoidal vibrator are captured by the receiver placed on the ground surface. The receiver is moved away from the source in a straight line to measure the wavelengths. At a given frequency, there can have many different positions of the receiver that their particle motions are in phase with the source. At a location of receiver, we will obtain the number of waves (in-phase) and the particular distance of receiver from the source, so that they can be plotted in a diagram proposed Richart et al. (1970) (figure 2-2).

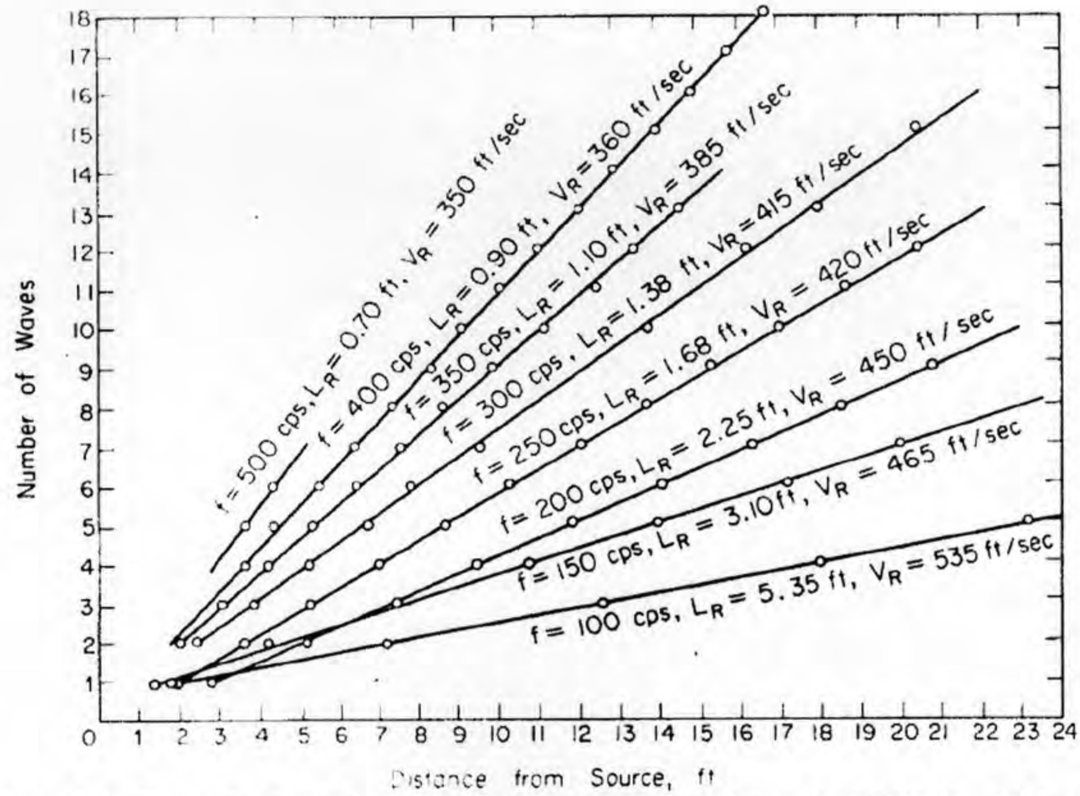

Figure 2-2 Determination of Average Wavelength of Rayleigh Waves by SSRM (from Richart et al. 1970)

By connecting the points, we get an incline line which its slope represents the inverse of wavelength for the current frequency. For example, the lowest line in figure 2-2 is composed of five different locations of the receiver at which the signals are in-phase with the input frequency 100cps from the source. Thus, the slope of the line or the inverse wavelength is equal to 5.35ft. Then from the wavelength λ_R and the input frequency *f*, the phase velocity of Rayleigh wave V_R is determined by:

$$V_R = f \cdot \lambda_R . \tag{2.1}$$

Once a pair of V_R and λ_R was determined, the characteristic dispersion curve (V_R vs. λ_R) can be constructed by varying the input frequency and determining the λ_R in the same manner.

In this approach, a direct conversion from V_R - λ_R domain to shear wave velocity - depth is performed by

$$V_S \approx 1.1\, V_R \tag{2.2}$$

$$z \approx \frac{\lambda}{3} \; or \; z \approx \frac{\lambda}{2}. \tag{2.3}$$

2.3 Spectral Analysis of Surface Wave Method (SASWM)

The idea of SSRM was extended to Spectral Analysis of Surface Wave Method (SASWM) during the Eighties by Heisey et al. (1982), Nazarian and Stokoe (1984), and Stokoe et al. (1988) to achieve more prolific testing. The development was possible because of the improvement in equipments such as the portable digital instruments and the tools for computing. The in situ testing became much faster and more reliable that made it popular topic to discuss. To obtain useful soil parameters from SASWM, three successive steps are needed, i.e., data acquisitions in the field, dispersion curve processing, and inversion.

2.3.1 Field Configuration

Instead of a single receiver used in SSRM, a couple of receivers are employed in SASWM. They are moved along a straight line on the ground surface away from the impulsive, sinusoidal, or random noise sources as shown in Figure 2-3. The source generates the incident Rayleigh waves with over a certain frequency range detected by the receivers and recorded into seismograph for further analysis by the microcomputer. The distance between the source and the first receiver is usually taken equal to that between the receivers. Based on the numerical simulation presented by Sanchez-Salinero (1987), the choice of this configuration is not a strict rule to follow, but it offers the balance between the influence of different factors (attenuation, spatial aliasing, near-field effects, etc.). The test is repeated several times by adjusting the positions between source-to-receiver and receiver-to-receiver to obtain a wide range of wavelengths and frequencies.

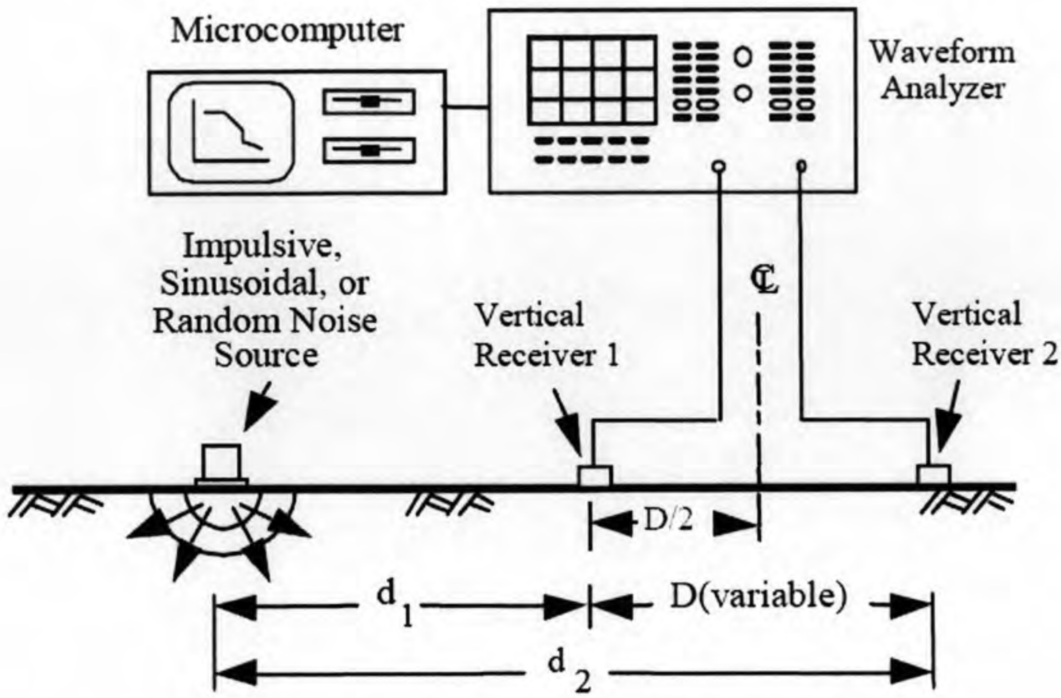

Figure 2-3 **SASWM field configuration (Stokoe et al., 1994)**

The length of the adjacent is configured in accordance with the source energy and the attenuation of signals by both geometric and material damping. A weak impulse sources such as a small hammer generates high frequency (short wavelengths) that fits with short receiver spacing (0.5-5m). The heavy sources (e.g. a massive weight drop or the movement of a bulldozer) will generate low frequency (long wavelengths) matches with long receiver spacing (up to 60m). Usually, there are two ways to move the receivers, one is common receiver midpoint array with source position reversing and another is common source array as shown in figure 2.4 and 2.5, respectively.

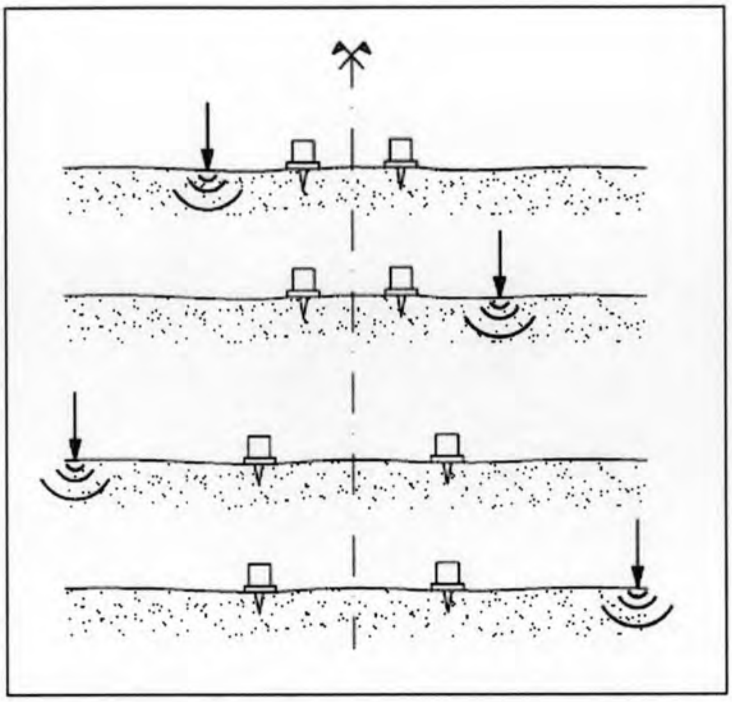

Figure 2-4 **Common Receiver midpoint array with source position reversing (Foti, 2000)**

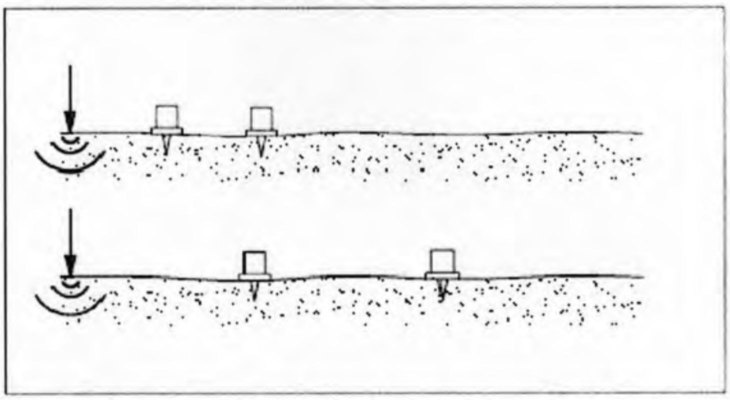

Figure 2-5 **Common Source array (Foti, 2000)**

The decision to choose one of these schemes essentially depends on the portability of the equipment used and the site condition. Practically, the common receiver midpoint array is preferred by the fact that it allows operator to verify the data by reversing symmetrically the position of the source to geophones midpoint. Besides, serving as a tool to compensate the phase distortion in the geophones, this method also figures out the lateral inhomogeneities and bedding inclination. Nevertheless, the inversion process in SASWM is strongly based on the hypothesis of plane and parallel layers.

2.3.2 Signal Processing and Dispersion Curve Construction

The dispersion curve (the phase velocity of Rayleigh wave as a function of frequency) is evaluated from the particle velocity or acceleration recorded at the geophones. Firstly, the signals in time domain (*y1(t)* and *y2(t)* in figure 2.6) are transformed into frequency domain (Y1(ω) and Y2(ω)) by the Fast Fourier Transform. During this step, the quality of the signals is judged by coherent function. The linear correlation between the input and output signals is a sign of good quality measurement which is not disturbed by the ambient noise.

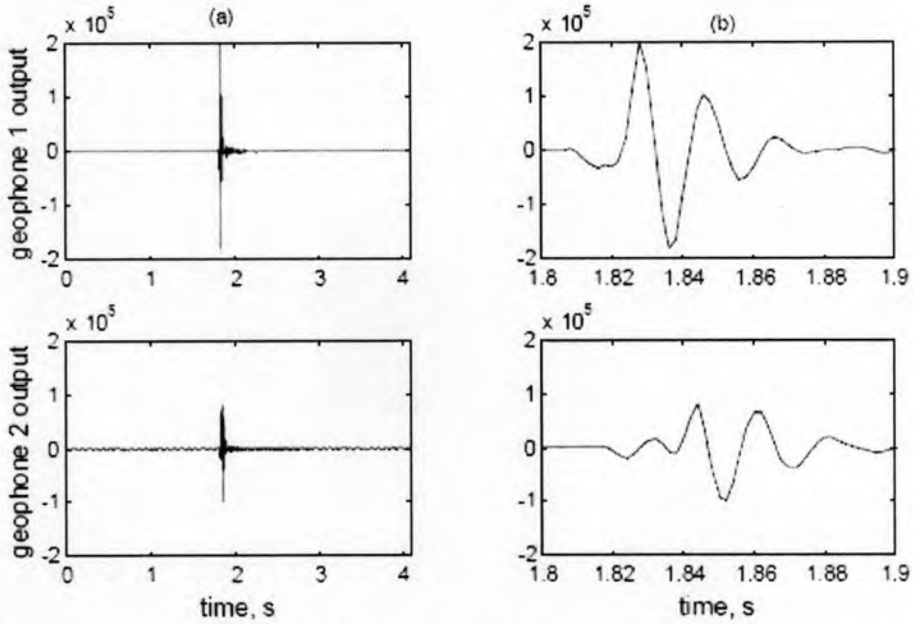

Figure 2-6 Example of SASW signals: (a) whole signals; (b) wave-train arrivals. (site: ENEA; source: 6kg hammer; d=2m) (Foti, 2000)

The procedure to obtain the dispersion curve depends on the following manipulations in frequency domain;

- Auto-power spectra (Figure 2.7c,d):

$$G_{11}(\omega) = Y_1(\omega).\overline{Y_1(\omega)} \tag{2.4}$$

$$G_{22}(\omega) = Y_2(\omega).\overline{Y_2(\omega)} \tag{2.5}$$

(where ¯ denotes the complex conjugate)

- Cross Power Spectrum:

$$G_{12}(\omega) = Y_1(\omega).\overline{Y_2(\omega)} \quad (2.6)$$

- Phase of Cross Power Spectrum (Figure 2.7a):

$$\Theta_{12}(\omega) = \tan^{-1}\left(\frac{Im\left(G_{12}(\omega)\right)}{Re\left(G_{12}(\omega)\right)}\right) \quad (2.7)$$

The Phase of Cross Power Spectrum is used to illustrate the phase shift between the signals from two different positions, and later to determine the time delay and phase velocity.

- Coherence function (Figure 2.7b):

$$\gamma_{12}^2(\omega) = \frac{G_{12}(\omega).\overline{G_{12}(\omega)}}{G_{11}(\omega).G_{22}(\omega)} \quad (2.8)$$

The quality of signals can be verified by checking the coherence function of a signal pair which varies from 0 to 1. When the value is closed to 1, the signals measured from the two geophones are well correlated with optimum signal to noise ratio. The value closed to zero indicates that the measurement is interfered by several factors such as body wave disturbance, noise, spatial variability, etc.

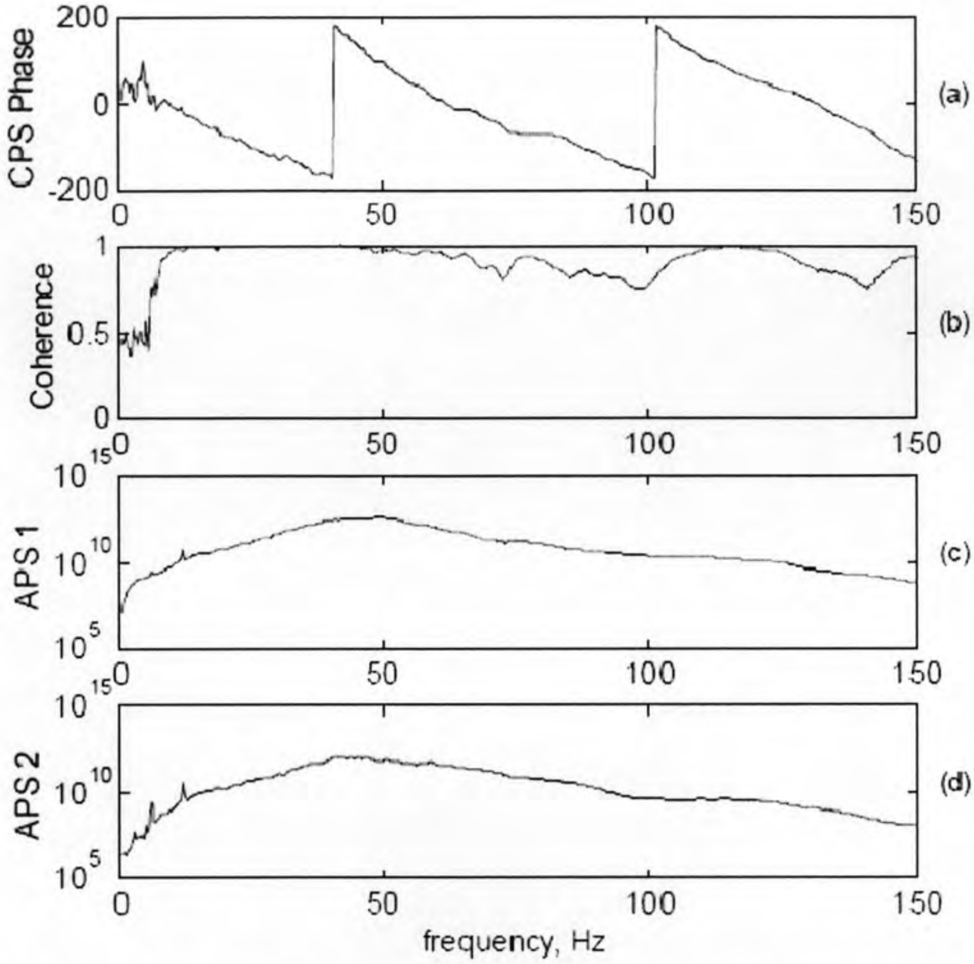

Figure 2-7 Spectral quantities evaluated from the signals of Figure 2.6 : (a) Phase of the cross-power spectrum; (b) Coherence function; (c) Auto-power spectrum (first receiver); (d) Auto-power spectrum (second receiver) (Foti, 2000).

- Time delay between the receivers:

$$t(\omega) = \frac{\Theta_{12}(\omega)}{\omega} \tag{2.9}$$

- Phase velocity of Surface waves:

$$V_R(\omega) = \frac{D}{t(\omega)} \tag{2.10}$$

where D is the distance between the two receivers.

- Wavelength:

$$\lambda_R(\omega) = \frac{V_R(\omega)}{f} \tag{2.11}$$

By following up the above successive calculation, the phase velocity as a function of frequency can be constructed and used in inversion process to get the shear wave velocity profile. But before going to the inversion step, it is important to understand the distinction between normal dispersion and inverse dispersion of the systems, which have the influences on the inversion algorithm.

2.3.3 Normally and Inversely Dispersive Systems

Firstly, the general definition of both the phase velocity and the group velocity should be brought up since these terminologies describe the characteristic of wave motions moving along the free surface. A group velocity of the signal composes of several single frequency signals, each one travelling with its own velocity. The system is said dispersive if the phase velocity varies according to the frequency. The normal dispersion or inverse dispersion behaviors are distinguished by the variation of the phase velocities inside the group velocity envelope (see figure 2-8). The normally dispersive system is defined when the phase velocity is greater than the group velocity. On the contrary, the phase velocity is less than the group velocity for inversely dispersive case.

Similarly, if the stiffness of the layered half-space media increases gradually with depth, the system is called normally dispersive (example in figure 2-9a). For the inversely dispersive system the stiffness varies irregularly with depth, sometimes softer layers sandwich the stiffer ones or vice versa softer layers are trapped between the stiffer ones (figure 2-9b). The concept of these two different systems is aroused to keep remind of their effects on the processing method.

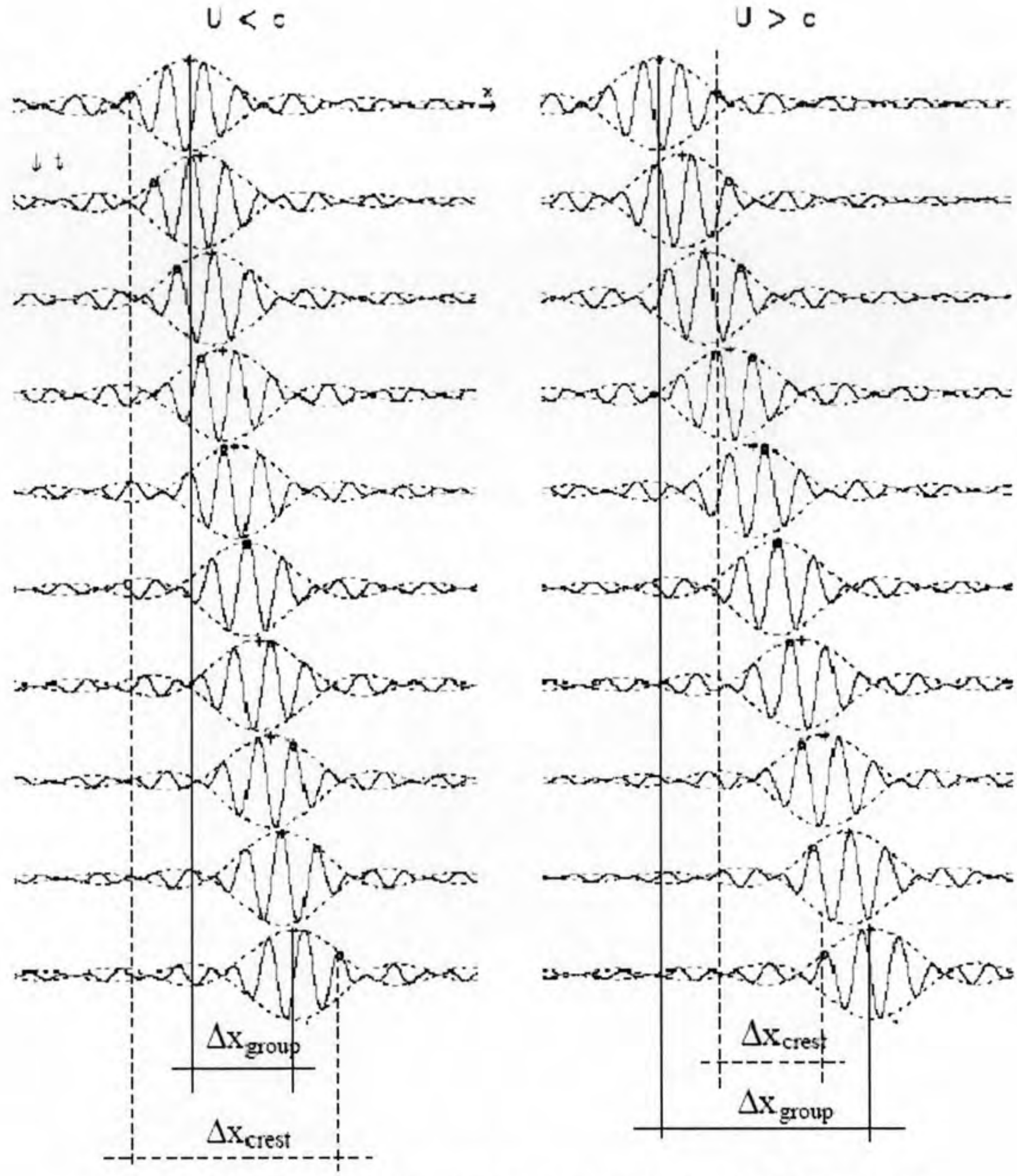

Figure 2-8 Normal and Inverse Dispersion Phenomenon (Roma, 2001)

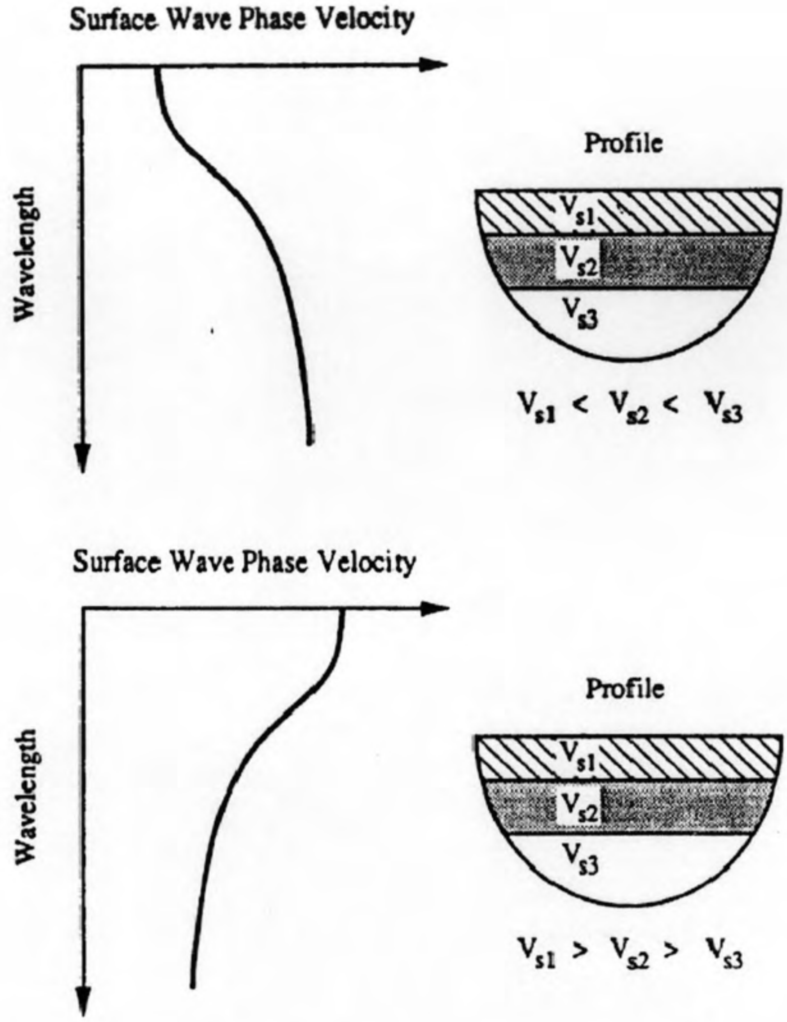

Figure 2-9 a, b: Normally and Inversely Dispersive layered half-spaces (Foti, 2000)